Journal of Sound and Vibration (1999) **220**(1), 99–115
Article No. jsvi.1998.1934, available online at http://www.idealibrary.com on IDEAL

ACTIVE CONTROL OF SOUND RADIATION FROM A RECTANGULAR PLATE EXCITED BY A LINE MOMENT

J.-C. Lee and J.-C. Chen

Dept. of Marine Engineering Technology, National Taiwan Ocean University, Keelung, Taiwan, Republic of China

(*Received* 27 *November* 1997, *and in final form* 19 *August* 1998)

This paper analytically investigates the active control of sound radiation from a simply supported rectangular plate with line moment excitation. This model simulates ship hull vibration due to the flutter of the ship's deck or the vibration of a fuselage due to the flutter of an aircraft wing. Two control strategies, volume velocity cancellation and radiated sound power minimization, are applied to drive a long and narrow piezoelectric actuator to reduce the radiated power. The result shows that a reduction of radiated power by these two control strategies is made possible by the mechanisms of modal suppression and modal restructuring. A numerical analysis shows that the performance of the active control method is related to the location of the line moment and an actuator. For the case in which the line moment is excited at the midline of the plate, the strategy of volume velocity cancellation is unable to reduce the sound radiated power. However, in the case where the actuator is located at the midline of the plate, both control strategies lead to the same reduction in radiated power except the control of the radiation of modes (even, 1). On the other hand, there exists a large amount of sound power radiation near the low frequency resonant mode (even, 1) when the line moment and the actuator are located off the midline of a plate and volume velocity cancellation is applied to control the radiated power from the plate.

1. INTRODUCTION

In many practical situations, the radiation of excessive noise power has been frequently observed in a plate-like structure, such as a panel or bulkhead. This noise power may be produced by plate vibrations and are originally induced by forces or dynamic moments exerted on the plate. The vibrations normally radiate excessive noise at the natural (or resonant) frequencies of the plate. This dynamic moment phenomenon is usually found in the ship and aircraft industries. In the first example, the harmonic excitation of a ship engine deck may generate a line moment at the bulkhead that connects the deck. In the second example, the airflow acting on a wing may result in a line moment at the fuselage. In the third, a harmonic line moment produced at the edge of two-layer composite structures may be observed.

0022–460X/99/060099 + 17 $30.00/0

In considering the prevention of noise nuisance, structurally radiated sound is a persistent problem. This problem is often poorly alleviated by passive means, particularly at low frequencies. The active control of sound radiation from a vibrating structure therefore becomes an important issue in the mitigation of low frequency machinery noise. Structural noise actively controlled using piezoelectric sensors and actuators, along with an effective control strategy has been studied by many researchers [1–4]. These studies point out that the control actuators, the error sensors, the control strategy and the electric controller determine the performance of active structural acoustic control.

Structural noise radiation is concerned with the coupling of the motions of elastic structures to their radiating sound fields. The power of radiated structural noise can be expressed in terms of the contributions of the velocity of a number of individually radiating elements of the plates' surface. This concept has been formulated and used to design either active or passive control methods [5, 6]. The distributed surface velocity of each individually radiating element is calculated using the eigenvectors of an elemental radiation resistance matrix. The independent radiating velocity distributions are referred to as the radiation modes of the surface. The radiation efficiencies of these radiation modes are proportional to the corresponding eigenvalues of the radiation resistance matrix.

To reduce the noise of structural vibration, one often tries to control the structural vibrating amplitude or the radiating efficiency using piezoelectric actuators or electromagnetic shakers. When an electromagnetic shaker is used as a control actuator, a reaction mount is required. This is because the electromagnetic shaker is heavy and cumbersome and especially impractical for lightweight structures. The piezoelectric actuators are usually bonded to or imbedded directly into the structure to eliminate many of the drawbacks of electromagnetic shakers. Clark *et al*. [7] developed a theoretical model of a simply supported beam configured with multiple piezoelectric actuators. He compared his analysis with his experimental results at a variety of frequencies, either on or off resonance. Dimitriadis *et al*. [8] derived equations for the excitation of two-dimensional structures along with piezoelectric actuators. Both Clark and Dimitriadis demonstrated that the piezoelectric actuators were able to excite selected modes of vibration in a distributed sense. Wang *et al*. [9] showed that properly selecting the pieces and location sites of piezoelectric actuators is critical to control noise radiation efficiently. The above literature demonstrates that the global control of the power of radiated noise from a vibrating structure could be achieved using piezoelectric elements as distributed actuators.

The control strategy is another important subject in active structural acoustic control. Two popular and well-known strategies for the active control of radiated power are volume velocity cancellation and radiated sound power minimization. Johnson and Elliott [5] demonstrated that the volume of the net velocity could be used to estimate the amplitude of the lowest radiation mode, which accounts for the majority of the sound power radiated in the low frequency region. Thus, the strategy of volume velocity cancellation can be a simple control strategy to achieve good active structural acoustic control in low frequencies without requiring a complex control system. It has also been reported [6] that a radiated sound power

minimization strategy performs best in an active feed-forward control system. However, that is difficult to implement practically.

Snyder and Hansen [10] investigated two physical mechanisms for active control of noise radiation from a baffled rectangular panel into free space: modal control (suppression) and modal rearrangement (restructuring). The importance of these two mechanisms depends on a variety of geometric and structural/acoustic system parameters. Several experiments conducted for active control of structurally radiated noise using multiple piezoelectric actuators have been reported recently [11, 12]. It is worth noting [12] that a three-channel adaptive controller based on a multichannel version of the Widrow–Hoff filtered-X control algorithm was implemented on a TMS320C25 DSP resident in an AT compatible computer. The adaptive LMS algorithm demonstrated that it was an effective narrow band controller, in contrast to the feedback approach, for which a little system modelling is required. All of the work described above demonstrates that the radiation directivity pattern and the plate vibrating distributions under the excitation of a point force or sound pressure are useful for evaluating the performance and mechanisms of the control. Unfortunately, up to now very little work has been done on the active control of noise radiation from a structure exhibiting line moment excitation.

This investigation attempts to evaluate the performance of active noise radiation control using a model of a simply supported rectangular plate excited by a line moment. It mimics the active control of noise radiation from a ship hull excited by a line moment from the flutter of the ship's deck. Also, this model is applicable to aircraft. It simulates the active control of noise radiation from a fuselage excited by a line moment from the flutter of the aircraft's wing. A line moment excited at different locations on a plate is considered to be a primary source, and a long and narrow piezoelectric patch to be a control actuator. The strategies of radiated sound power minimization and volume velocity cancellation are used to optimize the complex voltage input to the piezoelectric actuator, which minimizes the power of the sound radiated from the plate.

2. SOUND RADIATED POWER

As referred to in Johnson's work [5], the sound power, w, radiated by a structure is generated by a number of radiator elements on the structure. At any single frequency, the vector of complex linear velocities of each of these elemental sources is denoted as $\vec{\mathbf{v}}$. The vector of complex sound pressure immediately in front of each source, $\vec{\mathbf{p}}$, produces:

$$\vec{\mathbf{p}} = [\mathbf{Z}]\vec{\mathbf{v}}, \tag{1}$$

where $[\mathbf{Z}]$ is a matrix of specific acoustic impedance relating the complex pressure to the complex velocity of each element. The sound power radiated from the array of elemental sources is proportional to the real part of the sum of the conjugate

complex velocities of each radiator multiplied by the corresponding sound pressure. This can be expressed as:

$$w = (S/2)R_e[\vec{\mathbf{v}}^{\mathrm{H}}\vec{\mathbf{p}}], \tag{2}$$

where S designates the area of each radiator element with equal size. Superscript, H, denotes the Hermitian transposes. Substituting equation (1) into equation (2) and rearranging yields:

$$w = (S/2)R_e[\vec{\mathbf{v}}^{\mathrm{H}}Z\vec{\mathbf{v}}] = \vec{\mathbf{v}}^{\mathrm{H}}[\mathbf{R}]\vec{\mathbf{v}}. \tag{3}$$

This equation provides a convenient way of calculating radiated power if the transfer impedance matrix Z of a vibrating plate is known. In equation (3), $\mathbf{R}$ is a real, symmetrical, positive definite matrix and equals $(S/2)\mathbf{R}_e[\mathbf{Z}]$. The matrix can further be diagonalized through orthogonal transformation and written as $\mathbf{R} = \mathbf{Q}^{\mathrm{T}}\mathbf{\Lambda}\mathbf{Q}$. In this expression Q is a real and unitary matrix of orthogonal eigenvectors, $\mathbf{\Lambda}$ is a diagonal matrix of eigenvalues λ_i, which are all positive real numbers. The equation (3) can then be written as:

$$w = \vec{\mathbf{v}}^{\mathrm{H}}\mathbf{Q}^{\mathrm{T}}\mathbf{\Lambda}\mathbf{Q}\vec{\mathbf{v}}. \tag{4}$$

The radiation mode vector, $\mathbf{y} = \mathbf{Q}\vec{\mathbf{v}}$, is the weighted sum of these orthogonal functions. The radiated sound power can then be described, using the radiation modes and the eigenvalues of the sound power-weighting matrix $\mathbf{R}$, as:

$$w = \sum_{i=1}^{N_e} \lambda_i |y_i|^2 \tag{5}$$

where N_e is the number of element radiators. Equation (5) indicates that the radiation modes radiate independently. Some of the eigenvalues λ_i may be so small as to contribute to the total acoustic power radiation. The shape of the radiation modes is found directly from the rows of the matrix $\mathbf{Q}$, which corresponds to the eigenvectors of the radiation matrix $\mathbf{R}$. The shape of the lowest radiation mode at low frequencies is almost uniform across the radiator; and hence, the amplitude of the lowest radiation mode is very nearly proportional to the net volume velocity of a plate.

3. PLATE VIBRATION DUE TO A LINE MOMENT

The response of a plate, due to a line moment varying harmonically with time and uniform magnitude M_0, can be analyzed using the Dirac delta function δ. The dimension of M_0 is in N m/m distributed across a simple supported rectangular plate along the line $x = x'$, as shown in Figure 1. Both line distributed moments about the x- and y-axes, respectively, can be expressed as:

$$M_x = M_0\delta(x - x')\,\mathrm{e}^{\mathrm{j}\omega t} \quad \text{and} \quad M_y = 0. \tag{6, 7}$$

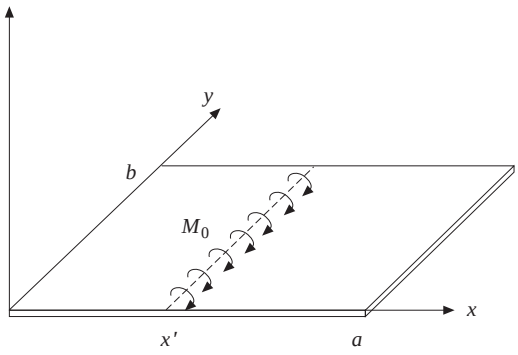

Figure 1. A rectangular plate with a line distributed moment excitation.

In equations (6) and (7), ω is the circular frequency, t the time, and $\mathrm{j} = \sqrt{-1}$. The modal expansion from Love's equation [13] may be written in terms of displacement u_i as:

$$L_1\{u_1, u_2, u_3\} - \lambda\dot{u}_1 - \rho h\ddot{u}_1 = 0, \qquad L_2\{u_1, u_2, u_3\} - \lambda\dot{u}_2 - \rho h\ddot{u}_2 = 0, \quad (8, 9)$$

$$L_3\{u_1, u_2, u_3\} - \lambda\dot{u}_3 - \rho h\ddot{u}_3 = -\partial M_x/\partial x. \quad (10)$$

A line dipole force, as given in the right term of equation (10), represents the line moment acting on the structure. The parameter, λ, in equation (10) again is the equivalent viscous damping factor, and ρh the mass density per unit of plate surface. The modal expansion series solution is:

$$u_i = \sum_{k=1}^{\infty} \eta_k U_{ik}, \quad (11)$$

where $i = 1, 2, 3$. The parameter, U_{ik}, stands for the natural mode components in the three principal directions. The modal participation factors η_k are determined through:

$$\ddot{\eta}_k + 2\zeta_k\omega_k\dot{\eta}_k + \omega_k^2\eta_k = F_k, \quad (12)$$

in which $\zeta_k = \lambda/2\rho h\omega_k$ is usually termed as the modal damping coefficient. For the transverse motion of a plate with a line moment, the steady state form of F_k can be expressed as:

$$F_k = (-4M_0 m/ab\rho hn)(1 - \cos n\pi)\cos(m\pi x'/a). \quad (13)$$

In equation (13), a and b give the dimensions of the plate in the x and y directions respectively. Again, in equation (13) the parameter m and n are mode numbers. It is worth noting that the vibrating mode is excited only when the value of the parameter n gives odd numbers in equation (13). The transverse displacement of the plate surface u_3 can then be described, through equation (11), as a sum of modes with sinusoidal mode shapes:

$$u_3(x, y) = \frac{8M_0}{ab\rho h} \sum_{n=1,3,\ldots,}^{\infty} \sum_{m=1}^{\infty} \frac{(m/n)\cos(m\pi x'/a)\sin(m\pi x/a)\sin(n\pi y/b)}{(\omega_{mn}^2 - \omega^2) + 2\mathrm{j}\zeta_k\omega_{mn}\omega}, \quad (14)$$

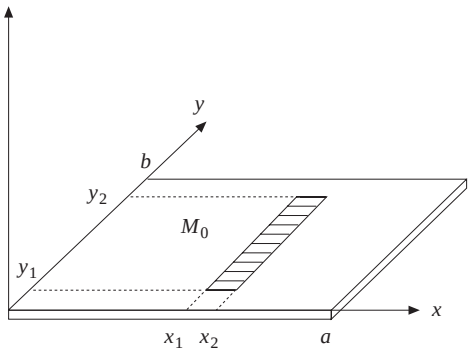

Figure 2. A piezoelectric actuator bonds on the plate.

where ω_{mn} is the natural frequency of the mode (m, n), which can be calculated from standard plate theory [14]. The velocity of an elemental source will be taken to be the plate velocity at the center of the corresponding elements. Plugging the co-ordinate values of the sites of the radiator elements into equation (14) and multiplying by $j\omega$ to convert displacement into velocity, one obtains:

$$v_i = \frac{8j\omega M_0}{ab\rho h} \sum_{n=1,3,\ldots,}^{M} \sum_{m=1}^{N} \frac{(m/n)\cos(m\pi x'/a)\sin(m\pi x_i/a)\sin(n\pi y_i/b)}{(\omega_{mn}^2 - \omega^2) + 2j\zeta_k\omega_{mn}\omega}, \quad (15)$$

where x_i and y_i are the co-ordinates of the ith element and M, N the numbers of modes in the modal summation.

4. PLATE RESPONSE DUE TO A PIEZOELECTRIC ACTUATOR

Two identical piezoelectric actuators, bonded perfectly and symmetrically on each side of the plate, are considered as control sources. The actuators, with their edges lined up with the edge of the plate, induce an internal moment across the piezoelectric actuators. As discussed by Dimitriadis *et al*. [8], the uniform distributed reaction moments in the plate are the result of the external line moments acting along the boundaries of the piezoelectric element. The response of the damped plate to the piezoelectric actuator with edge defined by x_1, x_2, y_1, y_2, as shown in Figure 2, can be expressed as:

$$u_e(x, y) = \frac{4C_0\epsilon_{pe}}{\rho hab} \sum_{n=1}^{\infty} \sum_{m=1}^{\infty} \frac{-([\alpha^2 + \beta^2]/\alpha\beta)(\cos\alpha x_1 - \cos\alpha x_2)(\cos\beta y_1 - \cos\beta y_2)}{(\omega_{mn}^2 - \omega^2) + 2j\zeta_k\omega_{mn}\omega}$$

$$\times \sin\alpha x \sin\beta y, \quad (16)$$

in which $\alpha = m\pi/a$, $\beta = n\pi/b$ and C_0 is the piezoelectric strain–plate moment coupling term [8]. In equation (16) the amplitude of the induced strains ϵ_{pe} can be expressed in terms of the piezoelectric strain constant, d_{31}, the applied voltage, V, and the actuator thickness, t_a

$$\epsilon_{pe} = (d_{31}/t_a)V. \quad (17)$$

The elemental velocity due to the piezoelectric actuator is available as given in equation (16). The total response of the plate will be a superposition of two parts: the vibration due to the external line moment and the vibration due to the piezoelectric actuator. To obtain desired responses, the control system will vary the applied voltage to the actuator so that the cost function is minimized.

5. THE STRATEGIES OF RADIATED SOUND POWER MINIMIZATION AND VOLUME VELOCITY CANCELLATION

The cost function that the control system seeks to minimize will be the total radiated acoustic power. The velocity distribution due to line moment, $\vec{\mathbf{v}}_M$, can be calculated from equation (15). The velocity distribution of the single piezoelectric actuator depends on the complex control signal $\mathbf{u}$ and the velocity response of the unit applied voltage $\vec{\mathbf{C}}$. The total velocity of the plate $\vec{\mathbf{v}}$ can be written as [5]:

$$\vec{\mathbf{v}} = \vec{\mathbf{v}}_M + \vec{\mathbf{C}}\mathbf{u}. \tag{18}$$

Substituting the velocity into the equation for sound power radiation, equation (3), the radiated power, w, gives:

$$w = u^{\mathrm{H}}\vec{\mathbf{C}}^{\mathrm{H}}\mathbf{R}\vec{\mathbf{C}}\mathbf{u} + \mathbf{u}^{\mathrm{H}}\vec{\mathbf{C}}^{\mathrm{H}}\mathbf{R}\vec{\mathbf{v}}_M + \vec{\mathbf{v}}_M^{\mathrm{H}}\mathbf{R}\vec{\mathbf{C}}\mathbf{u} + \vec{\mathbf{v}}_M^{\mathrm{H}}\mathbf{R}\vec{\mathbf{v}}_M. \tag{19}$$

This equation is of standard Hermitian quadratic form. Since $\mathbf{R}$ is positive definite, the cost function of w has a unique minimum value for a complex control signal given using:

$$\mathbf{u} = \mathbf{u}_{\mathrm{opt}} = -[\vec{\mathbf{C}}^{\mathrm{H}}\mathbf{R}\vec{\mathbf{C}}]^{-1}\vec{\mathbf{C}}^{\mathrm{H}}\mathbf{R}\vec{\mathbf{v}}_M. \tag{20}$$

The minimum radiated power under the control of the complex control signal $\mathbf{u}_{\mathrm{opt}}$ will then be:

$$w_{min} = \vec{\mathbf{v}}_M^{\mathrm{H}}\mathbf{R}\vec{\mathbf{v}}_M - [\vec{\mathbf{C}}^{\mathrm{H}}\mathbf{R}\vec{\mathbf{v}}_M]^{\mathrm{H}}[\vec{\mathbf{C}}^{\mathrm{H}}\mathbf{R}\vec{\mathbf{C}}]^{-1}[\vec{\mathbf{C}}^{\mathrm{H}}\mathbf{R}\vec{\mathbf{v}}_M]. \tag{21}$$

Accordingly, the radiated sound power minimization performs best at a single, defined excitation frequency for a given feed-forward control system.

The volume velocity cancellation is the other control strategy for driving the plate average volume velocity to zero. The net complex volume velocity $\mathbf{G}$ of the plate is the sum of the complex velocities at each of the elemental positions, $\vec{\mathbf{v}}$, multiplied by the elemental area, s. It can be written as:

$$\mathbf{G} = s\vec{\mathbf{v}}. \tag{22}$$

Substituting equation (18) into equation (22) gives

$$\mathbf{G} = s\vec{\mathbf{v}}_M + s\vec{\mathbf{C}}\mathbf{u}. \tag{23}$$

The optimal complex control signal can be found by setting the value of $\mathbf{G}$ to zero for the volume velocity cancellation. It then will be:

$$\mathbf{u} = \mathbf{u}_G = -s\vec{\mathbf{v}}_M/s\vec{\mathbf{C}}. \tag{24}$$

In equation (24) the complex control signal $\mathbf{u}_G$ does not drive the velocity of the plate to zero at any point. The attenuation of the total acoustic power radiation

TABLE 1

The physical properties of steel and the piezoelectric actuator

	Steel	Actuator
Density (Kg/m^3)	7870	7650
Poisson's ratio	0·29	0·30
Young's modulus (N/m^3)	207×10^9	63×10^9
d_{31} (m/V)		-166×10^{-12}
Thickness t_a (mm)		0·19

from this strategy will then be less than that obtained from the strategy for total radiated sound power minimization. The results given by these two control strategies are compared in the following section.

6. NUMERICAL RESULTS AND DISCUSSION

The results of computer simulations for the active control of sound radiation from a rectangular thin elastic plate excited by a line moment will be presented. In this simulation, the piezoelectric patch is considered to be an actuator. The amount of control of the sound power radiated, before and after the piezoelectric patch is applied, was compared with each other. The following discussion involves the strategies of radiated sound power minimization and volume velocity cancellation. Both strategies are designed to drive the piezoelectric patch to control the radiated sound power of the plate. For the reader's convenience, the physical properties of the steel plate and the piezoelectric actuator were prepared, as shown in Table 1. A plate with dimensions of $a = 0{\cdot}45$ m, $b = 0{\cdot}3$ m and $h = 2$ mm, whilst a damping of $\zeta_k = 0{\cdot}005$ was utilized for all cases. The resonant frequencies for modes (m, n) of the simply supported plate were calculated as shown in Table 2. Theoretically, active control is applicable for controlling multiple primary sources using multiple secondary sources. However, to simplify the present case, a single actuator along with a single harmonic line moment, M_0, whose value equals 10 N m/m was considered in this work. It was assumed that the plate was radiating into the air in this study. Both the radiated sound power and plate vibrating

TABLE 2

The resonant frequencies of a simply supported plate

	n				
m	1	2	3	4	5
1	78·1	240·3	510·6	889·0	1375·6
2	150·2	312·4	582·7	961·1	1447·6
3	270·3	432·5	702·8	1081·2	1567·8
4	438·5	600·7	871·0	1249·4	1736·0
5	654·7	816·9	1087·2	1465·7	1952·2

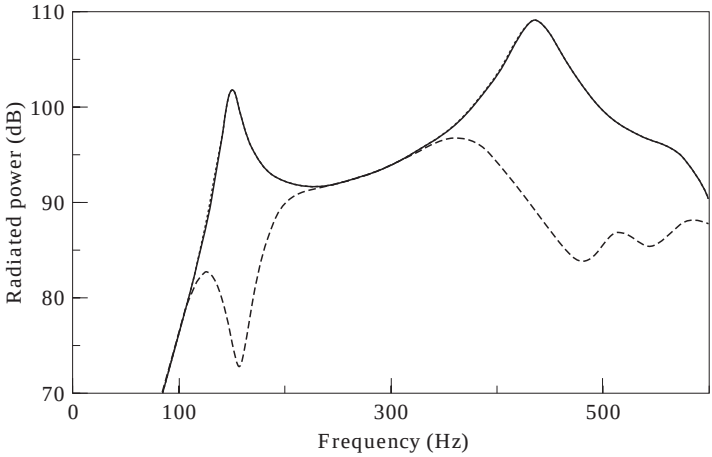

Figure 3. The sound power radiation from the plate excited by a line moment at $x = a/2$ midline. Key: before control (solid); after the radiated sound power minimization (dashed); after the volume velocity cancellation (dotted) as a function of frequency.

velocity distribution were used to discuss the effectiveness of the sound radiation active control. All results are plotted in two types: (1) radiated sound power versus frequencies before and after the active control, and (2) the normalized amplitude of the plate's vibration velocity distribution along the x-axis at $y = b/2$. The peaks observed in the radiated power before control are attributed to modal resonance. The radiated power is usually expressed in dB (ref: 10^{-12} W). In all plots, the solid lines indicate the results for the case without any control, the dashed lines, control by radiated sound power minimization and the dotted lines, control by volume velocity cancellation. The mode numbers $M = 10$ and $N = 10$ (100 modes) were used in this analysis. For the case of low frequency excitations, sufficient convergence was provided for the modal summation in equations (14)–(16).

Generally speaking, there are two ways to alter the plate's velocity distribution and furthermore, reduce the radiated sound power. They are modal suppression and modal restructuring. The modal suppression is simply a reduction in the velocity levels of the principal offending modes. The modal restructuring involves a shift in the contribution of the structural modes from well-radiating low order modes to higher order poorly radiating modes. In the following sections, three locations for the line moment excitation are chosen to show the performance of active control using the two control strategies with piezoelectric actuators at different locations.

6.1. LINE MOMENT EXCITING ALONG THE $x' = a/2$ VERTICAL PLATE MIDLINE

This section is concerned with a line moment excited at the position $x' = 0{\cdot}225$ m along the vertical plate midline. The location and the size of the piezoelectric actuator are $x_1 = 0{\cdot}05$ m, $x_2 = 0{\cdot}09$ m, $y_1 = 0{\cdot}04$ m, $y_2 = 0{\cdot}26$ m as in Figure 2. The radiated sound power of a vibrating plate due to low frequency line moment excitation before and after control by the two strategies in terms of a long and narrow piezoelectric actuator is shown in Figure 3. Figures 4(a–d) show the

plate's vibrating velocity distribution along the horizontal plate midline ($y = b/2$) for four resonance frequencies. In Figure 4(a), the structural modes (odd n) with a non-zero net volume velocity do not appear because of the central excitation of the line moment. This figure demonstrates the response of the plate's vibration with the second mode (2, 1), which was excited at the first resonance frequency (80 Hz). Similarly, Figure 4(c) gives the response of the plate's vibration with the fourth mode (4, 1), which was excited at the third resonance frequency (270 Hz). Based on observation from Figures 4(a) and 4(c), it can be stated that the radiated sound power is composed of structural modes (even n) associated with the non-volumetric modes. As shown in Figure 4, the net volume velocity of the plate's structural non-volumetric modes is inherently zero before the active control. There exists no radiated power reduction for driving the actuator at any location with the control strategy of the volume velocity cancellation. This result is clearly given in Figures 3 and 4, in which the solid curves overlay the dotted curves. Alternatively, the control strategy of radiated sound power minimization alters the amplitudes and phases of the mode velocities near the resonance frequencies 150 and 440 Hz as shown in Figures 4(b, d). These observations reveal that a substantial reduction of radiated sound power near the resonance frequencies can be found from the dashed curve in Figure 3. According to the previous discussion, the conclusion can be drawn that the control strategy of the volume velocity cancellation is unable to reduce the sound radiation of a plate with a line moment excited at its midline.

6.2. LINE MOMENT EXCITING ALONG THE EDGE OF THE PLATE

In this section, a plate excited by a line moment at its edge ($x' = 0$ m) and controlled by an actuator at two different locations will be discussed.

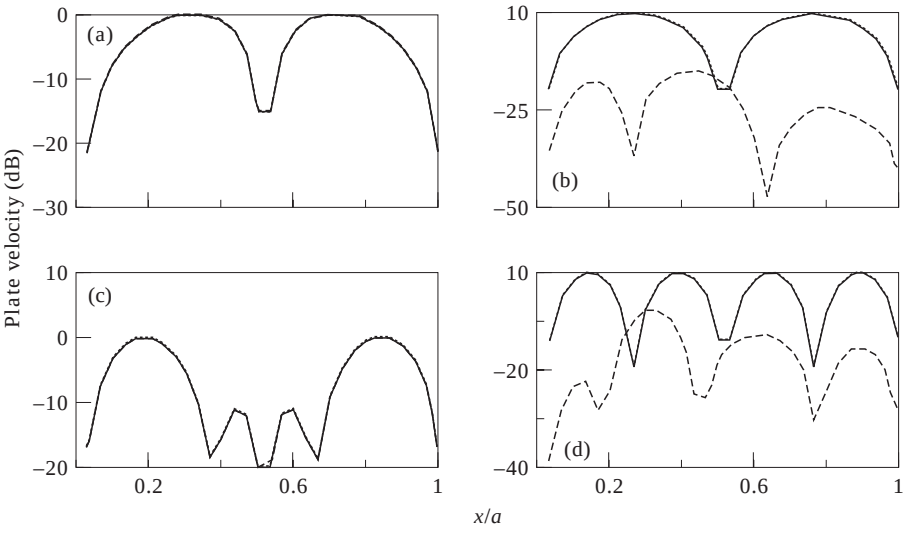

Figure 4. The plate vibrating velocity distribution along $y = b/2$ midline at resonance frequency: (a) 80 Hz; (b) 150 Hz; (c) 270 Hz and (d) 440 Hz. Key as for Figure 3.

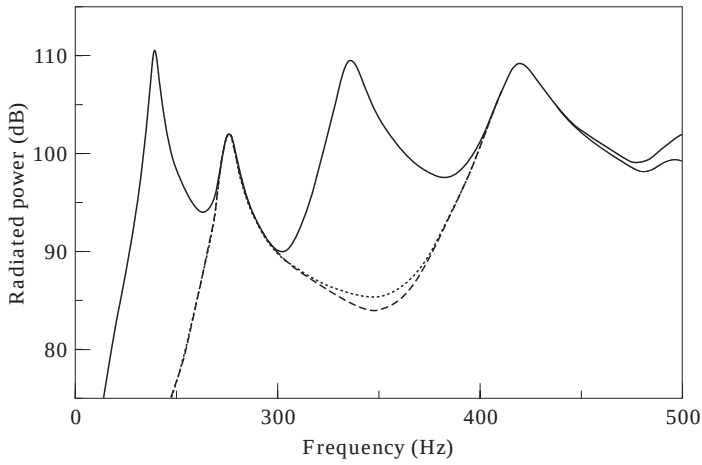

Figure 5. The sound power radiation from the plate excited by a line moment at the edge ($x = 0$). Key as for Figure 3.

Figure 5 shows the plate responses of the line moment excitation at resonance frequency 80 Hz which is dominated by the (1, 1) modes. Similarly, Figures 6–8 give the plate responses of the line moment excitation at resonance frequencies of 150 Hz, 270 Hz and 440 Hz which are dominated by the modes (2, 1), (3, 1), and (4, 1) respectively. In the other modes, a small amount of response as compared with the dominant resonant modes can also be observed at the resonance frequency excitation. The curves shown in Figures 5 and 6 present the control results for the actuator locating at $x_1 = 0{\cdot}205$ m, $x_2 = 0{\cdot}245$ m, $y_1 = 0{\cdot}04$ m, $y_2 = 0{\cdot}26$ m (the plate vertical midline). It is of interest that no obvious difference

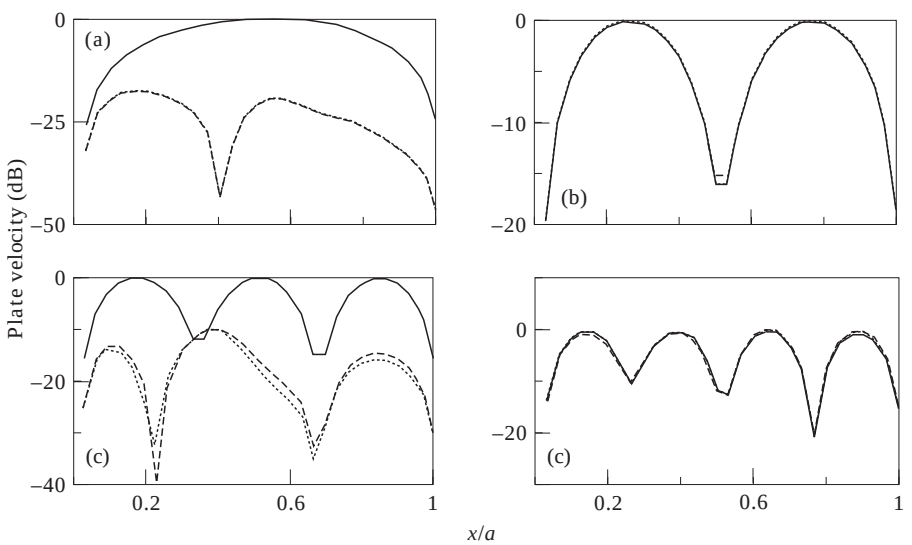

Figure 6. The plate vibrating velocity distribution along $y = b/2$ midline at resonance frequency: (a) 80 Hz; (b) 150 Hz; (c) 270 Hz; (d) 440 Hz; and with an actuator at the vertical midline. Key as for Figure 3.

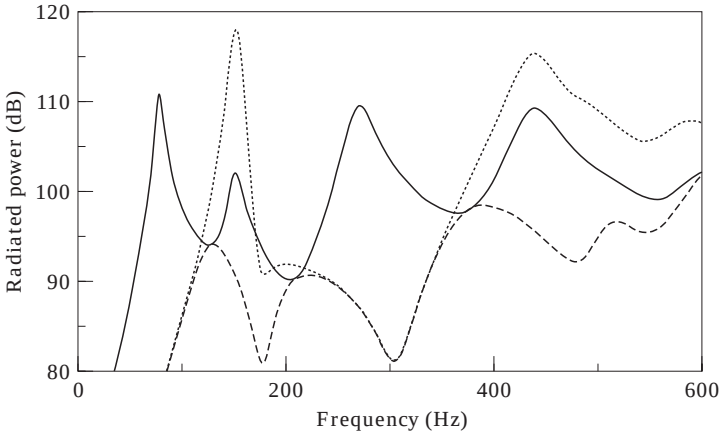

Figure 7. The sound power radiation from the plate excited by a line moment at the edge ($x' = 0$). Key as for Figure 3.

in the degree of reduction of the sound power radiation between radiated sound power minimization and volume velocity cancellation. This explains why the dotted and dashed lines in Figures 5 and 6 approximately match each other. In Figure 6(a) both control strategies in terms of the actuator suppress the (1, 1) mode and cause the (2, 1) mode with lower radiation efficiency to be the dominant mode. Therefore, a substantial radiated sound power reduction is observed at the 80 Hz frequency, as shown in Figure 5.

Figure 6(c) demonstrates that there is only a reduction in mode amplitude in the control of modes (3, 1). This agrees with the reduction of the radiated power

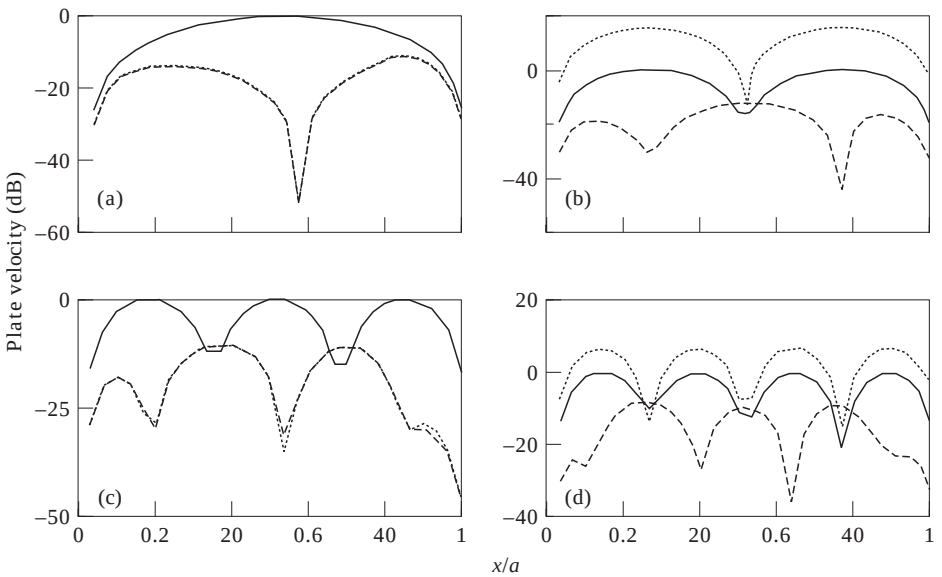

Figure 8. The plate vibrating velocity distribution along $y = b/2$ midline at resonance frequency: (a) 80 Hz; (b) 150 Hz; (c) 270 Hz; (d) 440 Hz; and with an actuator at $x = 0{\cdot}36$ m, $x = 0{\cdot}40$ m. Key as for Figure 3.

by about 25 dB at 270 Hz given in Figure 5. On the other hand, Figures 6(b, d) present no significant amplitude suppression and modal reconstructing for modes (2, 1) and (4, 1) after applying the two control strategies. Thus no radiated power at the second resonance frequency 150 Hz and at the fourth resonance frequency 440 Hz is observed in Figure 5. Based upon the statement as presented previously, it is reasonable for one to conclude that an actuator being driven by either strategy at the midline of the plate makes the same reduction in radiated power at the low frequency range. However, there is no radiated power reduction at all for the control of non-volumetric velocity modes (even, 1).

The results in Figures 7 and 8 show both control strategies and actuators located at $x_1 = 0{\cdot}36$ m, $x_2 = 0{\cdot}40$ m, $y_1 = 0{\cdot}04$ m, $y_2 = 0{\cdot}26$ m. Figure 8 presents the plate vibrating velocity distribution corresponding to the four resonance frequencies given in Figure 7. As expected, the $(m, 1)$ modes dominate the plate vibration (the solid line in Figure 8) because the line moment is excited near their resonance frequency. When the actuator is employed, as shown in Figures 8(a, c), the (odd, 1) mode is well controlled by these two control strategies. The result is that the remaining dominant radiating mode is the higher order mode (even, 1), which is characterized by a lower vibrating velocity amplitude and radiation efficiency. Accordingly, the significant reduction in radiated power after implementing the two control strategies in Figure 7 appears at resonance frequencies 80 and 270 Hz. On the contrary, for the case of resonance modes (even, 1), a substantial reduction in radiated power can be achieved using the control of radiated sound power minimization, as shown in Figures 8(b, d). However, with the control strategy of volume velocity cancellation, when the actuator is driven to cancel the small amount of volume velocity modes excited by the line moment at the frequency of 150 Hz, the actuator also strongly resonates in an excitation with mode (2, 1) at this frequency. Hence, the mode vibrating velocity amplitude after control is higher than before control, as shown in Figure 8(b). Also, significant amounts of sound power will radiate at 150 Hz, which can be found at the dashed line in Figure 7. This phenomenon can also be expected for mode (4, 1) at frequency 440 Hz, as shown in Figures 7 and 8(d).

Note that the effectiveness of active control using the strategy of radiated sound power minimization in the reduction of sound radiated power is not only in suppressing the mode amplitude but also in reconstructing the high order modes which possess lower radiated efficiency. Therefore, a significant difference between the solid and dashed curves can be found in Figures 7 and 8. The results for a harmonic edge line moment are important in the sound radiation of composite structures, such as two plates joined together at a single edge.

6.3. LINE MOMENT EXCITING ALONG $x' = 0{\cdot}36$ m OF THE PLATE

Figures 9 and 10 show the reduction of sound radiation from a vibrating plate with a line moment excited along $x' = 0{\cdot}36$ m and simultaneously using an actuator located at the vertical midline. The results as presented in section 6.2 for the actuator at the midline are also valid in this section. First, the two control strategies at low frequencies have the same sound power reduction, which is in good agreement between the dotted and dashed curves in Figures 9 and 10.

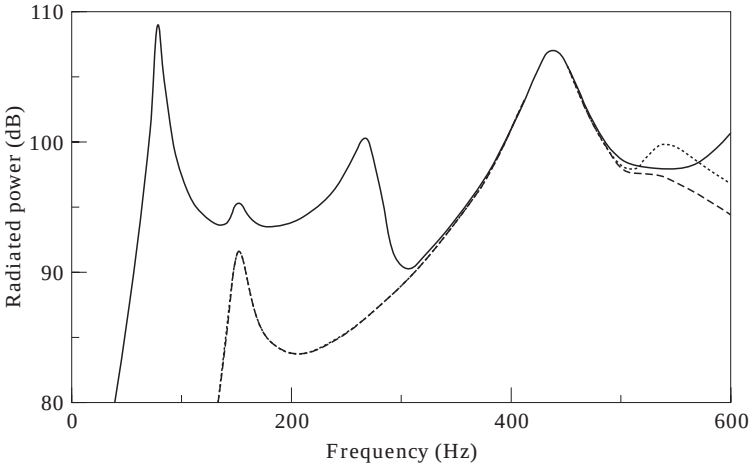

Figure 9. The sound power radiation from the plate excited by a line moment at $x' = 0{\cdot}36$ m. Key as for Figure 3.

Second, the two control strategies are unable to control the radiation of mode (even, 1) and therefore, the three curves in Figures 10(b, d) match one another. This observation makes no significant difference between the solid line and the other two curves in Figure 9, especially at a frequency of 440 Hz. However, in Figures 10(a, c) the mode (odd, 1) is suppressed and reconstructed to become a higher order mode (even, 1) so that the obvious reduction of radiated sound power can be achieved at the frequencies of 80 Hz and 270 Hz in Figure 9.

In the case where the control actuator is located at $x_1 = 0{\cdot}36$ m, $x_2 = 0{\cdot}40$ m, $y_1 = 0{\cdot}04$ m and $y_2 = 0{\cdot}26$ m, the plate vibrating velocity distribution corresponds

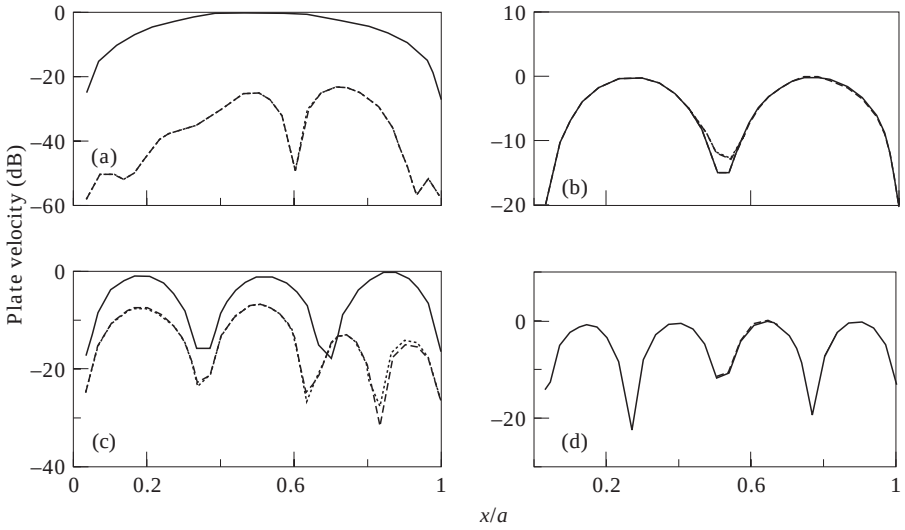

Figure 10. The plate vibrating velocity distribution along $y = b/2$ midline at resonant frequency (a) 80 Hz; (b) 150 Hz; (c) 270 Hz; (d) 440 Hz; and with an actuator at the vertical midline. Key as for Figure 3.

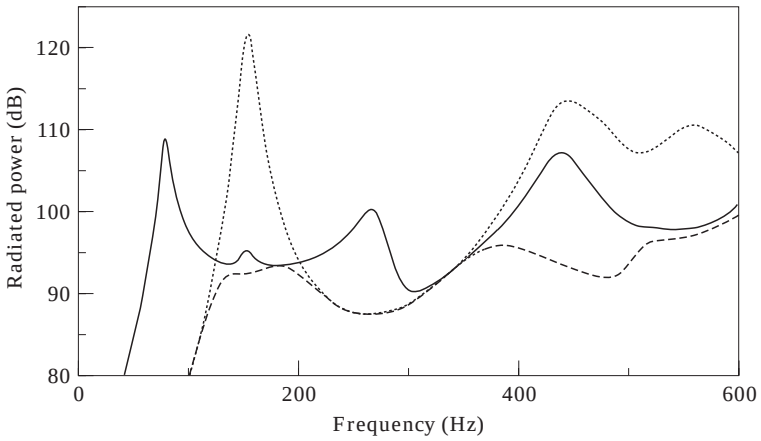

Figure 11. The sound power radiation from the plate excited by a line moment at $x = 0{\cdot}36$ m. Key as for Figure 3.

to the four given frequencies, namely 80 Hz, 150 Hz, 270 Hz and 440 Hz, provided in Figures 11 and 12. The resonant response of a plate excited by a line moment and an actuator at any location rather than the midline is composed of the dominant resonance mode and a smaller amount of other modes. As stated in section 6.2, using the strategy of volume velocity cancellation at a resonance frequency of 150 Hz, when the actuator intends to drive substantially small volume velocity modes for cancelling the volume velocity from a line moment excitation, the dominant resonant mode (2, 1) will also be excited strongly. The dotted line is, therefore, higher than the solid line in Figure 12(b) and the same result is observed at 150 Hz in Figure 11. This phenomenon is also found in resonance

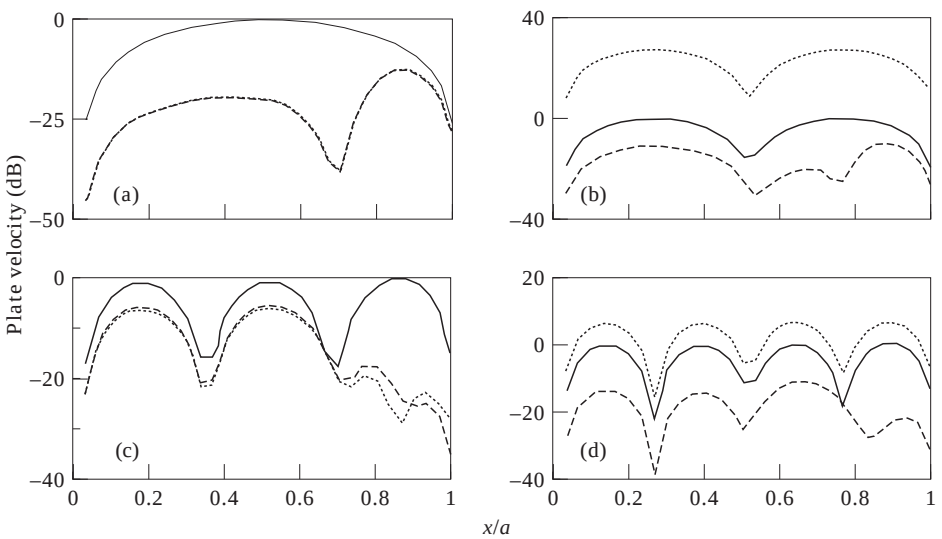

Figure 12. The plate vibrating velocity distribution along $y = b/2$ midline at resonant frequency: (a) 80 Hz; (b) 150 Hz; (c) 270 Hz; (d) 440 Hz; and with an actuator at $x = 0{\cdot}05$ m, $x = 0{\cdot}09$ m. Key as for Figure 3.

mode (4, 1). This leads to the result that the dotted line (after the control of the volume velocity cancellation) is higher than the solid line (before the control of the volume velocity cancellation) in Figures 12(b, d). Regarding the active control of the non-zero volume velocity resonant mode (1, 1) when excited at resonance frequency of 80 Hz, both control strategies suppress this mode and reconstruct to become a higher order mode (2, 1), as shown in Figure 12(a). Similarly, in the active control of resonance mode (3, 1) excited at 270 Hz, both control strategies suppress this mode and reconstruct to become a higher order mode (4, 1) again, as shown in Figure 12(c). It is quite evident, based upon the previous discussions, that modal suppression and modal restructuring are the significant mechanisms of the active control radiated power from a rectangular plate with line moment excitation.

7. CONCLUSIONS

Upon consideration of the present analysis, it can be stated that active control of sound radiation from a plate excited by a line moment depends upon the location of the line moment and the control actuator. Modal suppression and modal restructuring are considered to be two significant control mechanisms of radiated sound power minimization and volume velocity cancellation. Several conclusions can be drawn as follows:

1. The strategy of volume velocity cancellation is unable to reduce sound radiation from a plate excited by a line moment, which is located at the midline of the plate.
2. When the actuator is at the midline of the plate, the presented strategies lead to the same reduction in radiated sound power at low frequencies; however, they do not reduce the radiated sound power of (even, 1) modes.
3. When a line moment and an actuator are simultaneously off the midline, a small number of non-zero volume velocity modes and the dominant mode (even, 1) are excited at the resonant frequency. When the actuator is driven, it attempts to cancel the amplitude of the non-zero volume velocity modes using the strategy of volume velocity cancellation. The dominant modes (even, 1) are strongly excited and radiate significant sound power at low frequencies simultaneously. Obviously, to eliminate the amplification of the dominant resonant mode (even, 1), the actuator should be placed near the midline of the plate for line moment excitation off the midline.
4. The effectiveness of these control strategies in the reduction of radiated sound power from modes $(m, 1)$ depends upon the site of the actuator.

ACKNOWLEDGMENT

We would like to acknowledge the financial support given to the work by the National Science Council of Taiwan, R.O.C.

REFERENCES

1. C. R. Fuller and A. H. von Flotow 1995 *IEEE Control Systems* 9–19. Active control of sound and vibration.
2. C. R. Fuller, C. A. Rogers and H. H. Robertshaw 1992 *Journal of Sound and Vibration* **157**, 19–39. Control of sound radiation with active/adaptive structures.
3. C. H. Hansen and S. D. Snyder 1997 *Active Control of Noise and Vibration*. London: E and FN Spon, Chapman and Hall.
4. C. R. Fuller, S. J. Elliott and P. A. Nelson 1996 *Active Control of Vibration*. New York: Harcourt Brace.
5. M. E. Johnson and S. J. Elliott 1995 *Journal of the Acoustical Society of America* **98**, 2174–2186. Active control of sound radiation using volume velocity cancellation.
6. S. J. Elliott and M. E. Johnson 1993 *Journal of the Acoustical Society of America* **94**, 2194–2204. Radiation modes and active control of sound power.
7. R. L. Clark, C. R. Fuller and A. Wicks 1991 *Journal of the Acoustical Society of America* **90**, 346–357. Characterization of multiple piezoelectric actuators for structural excitation.
8. E. K. Dimitriadis, C. R. Fuller and C. A. Roger 1991 *Transactions of ASME* **113**, 100–107. Piezoelectric actuators for distributed vibration excitation of thin plates.
9. B. T. Wang, C. R. Fuller and E. K. Dimitriadis 1991 *Journal of the Acoustical Society of America* **90**, 2820–2830. Active control of noise transmission through rectangular plates using multiple piezoelectric or point force actuators.
10. S. D. Snyder and C. H. Hansen 1991 *Journal of Sound and Vibration* **147**, 519–525. Mechanisms of active noise control by vibration sources.
11. C. R. Fuller, C. H. Hansen and S. D. Snyder 1991 *Journal of Sound and Vibration* **150**, 179–190. Experiments on active control of sound radiation from a panel using a piezoelectric actuator.
12. R. L. Clark and C. R. Fuller 1992 *Journal of the Acoustical Society of America* **91**, 3313–3320. Experiments on active control of structurally radiated sound using multiple piezoceramic actuators.
13. W. Soedel 1993 *Vibrations of Shells and Plates*. Marcel Dekker, 270 Madison Avenue, New York.
14. A. Leissa 1973 *Vibration of Plates* (*NASA* SP160). Washington D.C.: U.S. Government Printing Office.